Catalysis Today 171 (2011) 192–200

Contents lists available at ScienceDirect

Catalysis Today

journal homepage: www.elsevier.com/locate/cattod

The impact of cobalt aluminate formation on the deactivation of cobalt-based Fischer–Tropsch synthesis catalysts

D.J. Moodley[a,*], A.M. Saib[a], J. van de Loosdrecht[a,b], C.A. Welker-Nieuwoudt[a], B.H. Sigwebela[a], J.W. Niemantsverdriet[b]

[a] Sasol Technology, Fischer Tropsch Catalysis Research, 1 Klasie Havenga Rd, P.O. Box 1, Sasolburg 1947, South Africa
[b] Schuit Institute of Catalysis, Eindhoven University of Technology, P.O. Box 513, Eindhoven 5600 MB, The Netherlands

ARTICLE INFO

Article history:
Received 25 October 2010
Received in revised form 21 March 2011
Accepted 28 March 2011
Available online 31 May 2011

Keywords:
Cobalt
Fischer–Tropsch
Deactivation
Cobalt aluminate
Oxidation
Reduction
XANES

ABSTRACT

It has been reported that cobalt aluminate formation is a cause of deactivation during Fischer–Tropsch synthesis (FTS), as it forms at the expense of active cobalt and is irreducible during FTS. To study this quantitatively, wax-coated $Co/Pt/Al_2O_3$ catalyst samples were removed periodically from an extended demonstration reactor FTS run operated at commercially relevant conditions and analysed with X-ray Absorption Near Edge Spectroscopy (XANES). With XANES, wax protected spent samples could be analysed in a "pseudo in-situ" mode. Under commercially relevant FTS conditions the catalyst undergoes reduction and minimal amounts of cobalt aluminate were found. It is proposed that the cobalt aluminate is formed from the residual CoO present in the catalyst after reduction. Additionally, the formation of aluminate was investigated with XANES and X-ray photoelectron spectroscopy (XPS) and TPR-MS on catalysts taken from laboratory continuous stirred tank reactor (CSTR) runs with varying water partial pressure (1–10 bar). Even at high water partial pressures (P_{H_2O} = 10 bar, P_{H_2O}/P_{H_2} = 2.2) only around 10% cobalt aluminate is formed while the metallic fraction of cobalt still increased compared to the fresh catalyst. The work shows that cobalt aluminate formation during FTS at realistic conditions is not a major deactivation mechanism.

1. Introduction

In the next few decades natural gas is expected to become an important raw material as an alternative to crude oil for the production of liquid fuels [1]. The Fischer–Tropsch synthesis (FTS) is an integral part of gas-to-liquids (GTL) technology, which involves the conversion of synthesis gas (H_2/CO), derived from natural gas, to liquid hydrocarbon fuels. These fuels have a low sulphur and aromatic content [2]. Cobalt-based catalysts are the preferred choice due to their high per pass conversion, selectivity towards linear hydrocarbons, and low selectivity towards CO_2 [3,4]. However, cobalt is an expensive metal and therefore high catalyst stability is desired. In order to optimise the usage of a cobalt catalyst for such processes, an understanding of the deactivation mechanisms at play is paramount.

The deactivation mechanisms mentioned in literature for cobalt-based catalysts include: poisoning of the cobalt surface by sulphur and nitrogen compounds [5,6]; oxidation of the metallic phase by product water to form an inactive oxidic fraction [7]; sintering of the active phase facilitated by the product water and the reaction conditions [8]; reconstruction of cobalt surface due to the intrusive nature of CO [9,10]; solid state transformation involving the diffusion of cobalt into the support to form irreducible cobalt support compounds (e.g. aluminates and silicates) [11,12] and the formation of inert carbon phases which can block the cobalt active phase [13–15]. From a Sasol perspective, it has been put forward that sintering, carbon deposition, poisons and possibly surface reconstruction contribute towards the deactivation of cobalt-based FTS catalysts while oxidation is not believed to play a role [15].

Due to the high costs of cobalt it is required that the catalyst has high dispersion and catalysts are thus designed with small cobalt nanoparticles (around 6 nm) well dispersed over a high surface area carrier like silica, titania or γ-alumina [4]. Co/Al_2O_3 catalysts are usually prepared by: (a) impregnation of cobalt (II) nitrate (b) thermal treatment in air to decompose the nitrate precursor and oxidise the cobalt to Co_3O_4 [16] and finally (c) reduction of the Co_3O_4 to metallic cobalt [16,17]. In the case of thermal treatment in air at high temperatures (>350 °C), it is possible for cobalt ions to diffuse into the support to produce cobalt support compounds which are only reducible at harsh conditions (>800 °C in H_2) [7]. It is known that Co_3O_4 and γ-alumina have isotopic crystal

* Corresponding author. Tel.: +27 16 960 7015; fax: +27 11 522 1229.
E-mail address: denzil.moodley@sasol.com (D.J. Moodley).

0920-5861/$ – see front matter © 2011 Elsevier B.V. All rights reserved.
doi:10.1016/j.cattod.2011.03.078

structures and this contributes to the ease of migration of ions from cobalt oxide into the support during these oxidative treatments [18]. Additionally the ionic radius of trivalent cobalt (0.063 nm) and aluminium (0.054 nm) are quite similar and during high temperature calcination it is possible that Co^{3+} ions from Co_3O_4 are gradually replaced by Al^{3+} to produce a series of spinel compounds which may include $CoAl_2O_4$ or $Co_2Al_2O_4$ [19]. It was also shown that during the reduction of Co/Al_2O_3 catalysts with hydrogen, water vapour is produced which results in the formation of a non-reducible cobalt aluminate-like spinel [20]. Considering all of the above it may be expected that fresh cobalt on alumina catalysts prepared via the above traditional route will contain a small amount of cobalt aluminate. For example, Wang and Chen [21] have shown by TPR that catalysts with 20 wt% Co/Al_2O_3 do have the presence of a cobalt aluminate phase. It was previously postulated that the interface could be a cobalt–aluminate type phase which stabilizes the cobalt crystallites on the support [22].

It is known from thermodynamic calculations by van Berge et al. [7] that bulk Co will not oxidise to CoO or Co_3O_4 during standard FTS conditions (P_{H_2O}/P_{H_2} = 1–1.5, P_{H_2O} = 4–6 bar), whereas the formation of metal-support compounds during the reaction such as cobalt aluminate is favourable. It is argued that the latter does not take place to a significant extent seeing as the formation of cobalt aluminate is kinetically hindered and proceeds via a CoO intermediate [7]. This is supported by work by Bolt [23] who showed that relatively severe hydrothermal treatment, i.e. steam at 500–800 °C, of Co/Al_2O_3 model catalysts is required for the further formation of cobalt aluminate.

Water is always present in the FTS due to the removal of adsorbed oxygen, which arises from the dissociation of CO on the metal surface, by hydrogen. The amount of water will vary depending on the choice of reactor, catalytic system and process conditions [24]. Commercially relevant FTS conditions (i.e. 230 °C, 20 bar, H_2 + CO conversion between 50 and 70%, feed gas composition of 50–60 vol.% H_2 and 30–40 vol.% CO) create water partial pressures in the range of 4–6 bar. In a slurry phase reactor at these conditions, high water concentrations and low reactant concentrations will exist throughout the entire reactor due to extensive back mixing [25]. The produced water will not be converted to CO_2 to an appreciable extent due to the low water gas shift activity of cobalt [3].

Water has been shown to increase the rate of metal aluminate formation [23] on a model catalyst consisting of cobalt evaporated onto polycrystalline γ-alumina. Various authors [11,27–29] have also claimed that high water partial pressure increases the formation of aluminate on cobalt-based catalysts either during FTS or at model conditions in mixtures of H_2/H_2O. Often the observed deactivation is ascribed to the formation of aluminate as it is proposed that the irreducible cobalt-support species is formed from/at the expense of active metallic cobalt.

Jacobs et al. [26] have shown using X-ray Absorption Near Edge Spectroscopy (XANES) that high levels of water (ca. 30 vol%, P_{H_2O}/P_{H_2} = 1.7), which occur at high conversions (due to low space velocity employed), resulted in an irreversible deactivation of platinum promoted Co/Al_2O_3 catalysts in the FTS due to the formation of a cobalt aluminate like species from small cobalt clusters. Hilmen et al. [29] also ascribed the deactivation observed under model conditions with their rhenium promoted Co/Al_2O_3 catalysts to the formation of a cobalt aluminate phase. The authors showed, using XPS and TPR, that at 250 °C, and at P_{H_2O}/P_{H_2} = 10, cobalt aluminate formation was favoured [29]. They also found cobalt aluminate in samples exposed to H_2O/He mixtures where P_{H_2O} = 5.5 bar.

Li et al. manipulated CO conversion by varying the space velocity over platinum promoted Co/Al_2O_3 catalysts during FTS in a CSTR [11]. They found an irreversible deactivation of the catalyst at high conversions and hence higher water partial pressures. They also co-fed water and reported that increasing the amount of added water to provide a P_{H_2O} = 8.35 bar and a ratio of P_{H_2O}/P_{H_2} = 0.59 in the feed resulted in a permanent deactivation of the catalyst. These observations, along with increased CO_2 selectivity led them to assume that either CoO or $CoAl_2O_4$ had formed at these conditions as these two compounds are believed to be WGS-active. Similarly Tavasoli et al. [29] showed recently that alumina-supported cobalt catalysts deactivated at higher reaction rates due to the high partial pressure of water. Rapid deactivation at 260 °C, 1 bar was noted for $P_{H_2O}/(P_{H_2} + P_{CO}) > 0.55$ and $P_{H_2O}/P_{CO} > 1.5$, which translates to $P_{H_2O}/P_{H_2} > 0.76$. They postulated that the water aided in the formation of irreducible cobalt aluminate which they claim was detected in the spent catalyst by TPR.

A recent review on the deactivation of cobalt catalysts also indicates that cobalt aluminate formation during FTS, although kinetically restricted is a plausible deactivation pathway and that its formation may possibly be influenced by water [30]. The general consensus based on literature thus far may lead one to conclude that cobalt aluminate formation is an important mechanism to consider during the deactivation of cobalt catalysts at realistic FTS conditions.

Various techniques have been used to detect cobalt aluminate and these include XPS [28], XRD [20], Raman spectroscopy [20] and TPR [21,28]. XRD fails to effectively differentiate between CoO and small amounts of cobalt aluminate while TPR, Raman spectroscopy and XPS are most useful for unused calcined catalysts. As an alternative, XANES is powerful technique that is able to differentiate between Co^0, CoO, Co_3O_4 and $CoAl_2O_4$ with a high sensitivity as compared to many other techniques. It has been used previously for the characterisation of used wax-coated cobalt catalysts [22,27]. The objectives of this study were to observe if appreciable amounts of cobalt aluminate will form during commercially relevant FTS conditions in an extended FTS run and to observe the effect of increasing water partial pressure on formation of cobalt aluminate and possibly relate this to the deactivation process.

This contribution forms part of series of papers examining the deactivation mechanisms in operation during an extended FTS run, following our earlier reports on (1) oxidation/reduction [22] (2) carbon deposition [14] and (3) sintering [37].

2. Experimental

2.1. Catalyst preparation

A 20 wt% Co/Al_2O_3 catalyst, promoted with 0.05 wt% platinum, was prepared by slurry impregnation of a γ-alumina support (Puralox 2/150 from Sasol Germany) with an aqueous cobalt nitrate solution, also containing the platinum promoter. After impregnation and drying, the catalyst intermediate was calcined at 250 °C in air and reduced in pure hydrogen at 425 °C. To achieve the required cobalt loading two impregnation and calcination steps were performed [31–36].

2.2. Characterisation of freshly reduced catalyst

The freshly reduced catalyst was previously analysed with high angle annular dark field transmission electron microscopy (HAADF-TEM) [37], hydrogen chemisorption, magnetic measurements and XANES [22,36]. Based on the results from these characterization techniques a model was obtained, describing the cobalt phases and crystallite size distribution for the freshly reduced catalyst prior to the FTS. As can be seen in Fig. 1, the cobalt crystallites have an average size of 6 nm [36,37]. It should be noted that the degree of reduction for a fresh catalyst is around 60%. A large portion of the unreduced material is believed to exist as small CoO crystallites

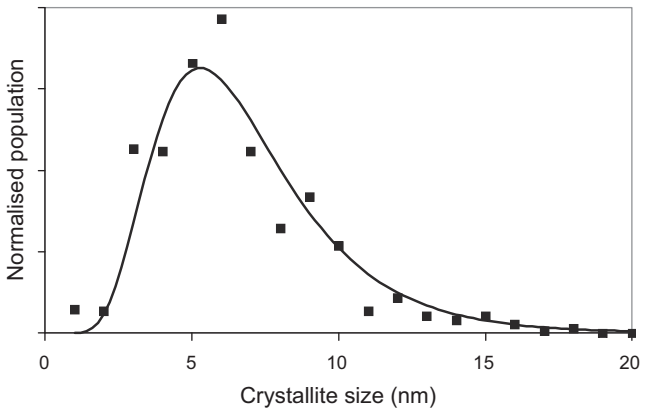

Fig. 1. Crystallite size distribution of cobalt for a freshly reduced $Co/Pt/Al_2O_3$ catalyst obtained with data from HAADF TEM [38].

(2–3 nm). It is also likely that some of the unreduced cobalt is due to close interaction with support, i.e. two layers of cobalt closest to the support. The layer closest to the support is in the form of a $CoAl_2O_4$ type phase

2.3. Catalyst testing

2.3.1. Demonstration unit run

A commercially prepared $Co/Pt/Al_2O_3$ catalyst was tested in a 100 bbl/day slurry bubble column reactor with a diameter of 0.9 m at commercially relevant FTS conditions, i.e. 230 °C, 20 bar, H_2 + CO conversion between 50 and 70%, feed gas composition of 50–60 vol.% H_2 and 30–40 vol.% CO direct comparison of catalyst performance can only be done at exactly the same realistic test conditions. As this is difficult to achieve experimentally, a model was developed using the Satterfield [38,39] equation, $r_{FT} = (kP_{H_2}/P_{CO})/(1 + kP_{CO})^2$, in which the observed catalytic performance can be recalculated to exactly the same test conditions. For this study the Relative Intrinsic (Fischer–Tropsch) Activity Factor (R.I.A.F.) was compared to an in-house prepared baseline catalyst. The activity data for this run is reported elsewhere [14].

2.3.2. Laboratory CSTR runs

Fischer–Tropsch synthesis tests were performed in a slurry-phase CSTR with a reactor volume of 670 ml. The catalyst samples (i.e. 10–30 g) were pre-reduced at 425 °C for 16 h in pure hydrogen at atmospheric pressure and a heating rate of 1 °C/min, and suspended, under an argon blanket, in 300 ml molten Fischer–Tropsch hydrogenated wax (Sasol H1 hard wax) inside the reactor. Realistic FTS conditions were employed, i.e. 230 °C, 20 bar, commercial synthesis gas as feed of composition: 50 vol% H_2, 25 vol% CO and 25 vol% inerts. The P_{CO} was kept at 4.0 ± 0.2 bar and P_{H_2} at 4.5 ± 0.2 bar while the P_{H_2O} was varied from 1 to 10 bar by adjusting the synthesis gas conversion and the total pressure. The synthesis gas flows were regulated by Brooks mass-flow controllers, and use was made of the ampoule-sampling technique as the selected synthesis performance monitoring method [40].

2.3.3. XANES sample preparation

The sample preparation was done as previously described in a glove box (0.1 ppm H_2O, 2 ppm O_2) to prevent oxidation of the cobalt [22]. Catalyst samples in wax were removed from the demonstration reactor at varying times-on-stream and at the end of each laboratory CSTR run and cooled down under nitrogen so as to maintain the integrity of the sample. XANES samples were prepared by pelletizing 40–50 mg of wax-coated cobalt catalyst removed from the reactor into a 1.3 cm^2 disc. The samples were sealed in Kapton tape and removed from the glove box prior to measurement. Previous benchmarking experiments with in situ and ex-situ reduced wax-protected samples showed that the sample preparation method does not introduce artificial oxidation [22].

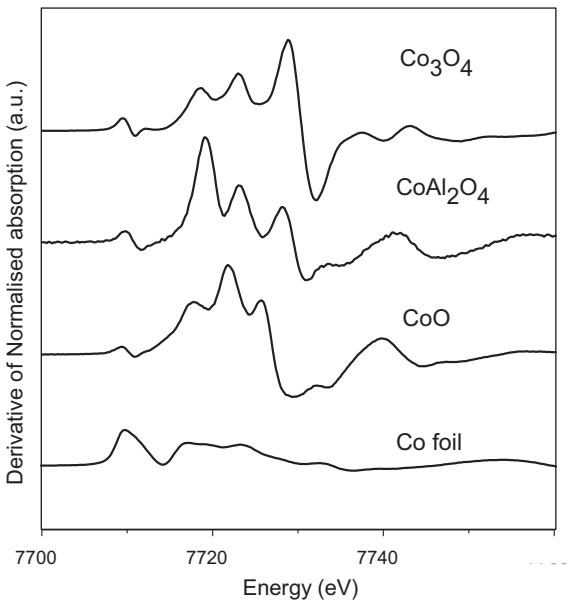

Fig. 3. XANES derivative spectra of reference compounds Co_3O_4, $CoAl_2O_4$, CoO and cobalt foil (Co^0).

2.3.4. XANES analyses of references and wax-coated catalysts

XANES measurements on reference compounds and wax-coated samples were performed at the ELETTRA synchrotron facility (Trieste, Italy) using a beam line with energy of 2–2.4 GeV. A double crystal monochromator (Si (1 1 1) and Si (3 1 1)) was used for varying the energy in the desired range. Measurements were carried out at the K-edge of Co. Calibration was performed with a Co foil using the first point of inflection of Co i.e. 7709 eV [41]. All spectra were recorded at liquid nitrogen temperatures. The XANES spectra were extracted from raw data by a conventional procedure. The pre-edge background was subtracted by using power series curves. Subsequently, the spectra were normalized by dividing by the height of the absorption edge. Spectra were quantified by fitting the experimental data with a weighted linear combination of reference compounds (Co^0, CoO, and $CoAl_2O_4$).

2.3.5. X-ray photoelectron spectroscopy analysis (XPS)

Samples of the spent catalysts tested at various water partial pressures, protected in a wax layer, were taken from the slurry-phase CSTR at the end of the reaction. The catalyst was allowed to congeal under an inert nitrogen environment. Due to the interference of this wax layer prior to XPS analysis, it was removed by an exhaustive reflux extraction with dry, deoxygenated tetrahydrofuran (THF, b.p. 66 °C) under an argon (99.999%) environment for around 3 h, using a P40 glass frit. After extraction the obtained catalyst particles were dried under vacuum at room temperature to remove the THF. The catalyst was then transferred under vacuum using Schlenk glassware into a glove box (2 ppm O_2, 0.1 ppm H_2O) for passivation. The samples were prepared in the glove box by crushing the wax-extracted FTS catalyst samples in a pestle and mortar. Afterwards, the powders were pressed into an indium layer on top of standard stainless steel XPS stubs and transferred via the glove box into the XPS pre-chamber.

The XPS measurements were carried out using a VG Escalab 200 MKII spectrometer. An aluminum anode (K_α = 1486.6 eV) was used

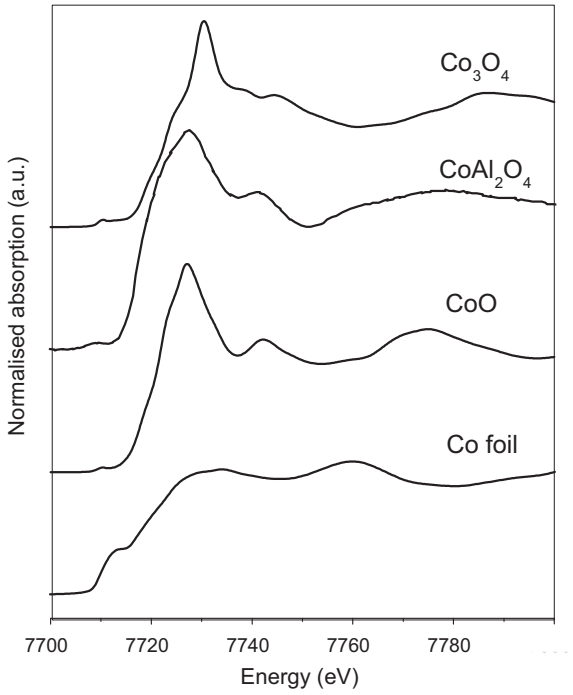

Fig. 2. XANES Co K-edge spectra of reference compounds Co_3O_4, $CoAl_2O_4$, CoO and cobalt foil (Co^0).

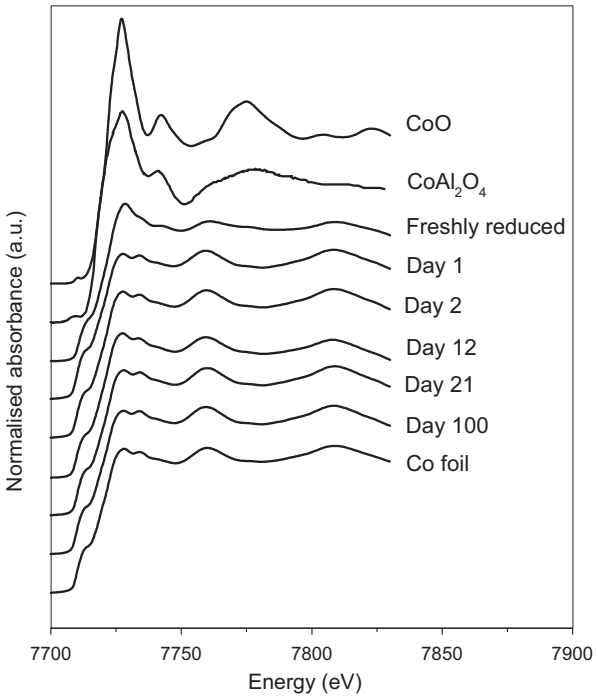

Fig. 4. XANES Co K-edge spectra of $Co/Pt/Al_2O_3$ catalyst taken at different intervals from an extended FTS and compared to reference compounds.

to generate the X-ray radiation (240 W (20 mA; 12 kV)). Measurements were carried out with a 0.1 s dwelling time; 0.1 eV step for the selected regions. To obtain sufficient signal-to-noise ratio the Co 2p region was scanned 80–120 times (i.e. making the total measurement approximately 3 h). During measurement the pressure in the main chamber remained below 10^{-8} mbar.

2.3.6. Temperature programmed reduction-mass spectrometry (TPR-MS)

Temperature Programmed Reduction (TPR) profiles of the catalyst were recorded on an Autochem 2920 (Micromeritics) instrument coupled with a MKS Cirrus Mass spectrometer. Approximately 100 mg of catalyst sample, as extracted as in Section 2.3.5 was placed in a U-shaped quartz tube fitted with a thermocouple for continuous temperature measurements. The sample was dried under helium flow (50 ml/min) by increasing the temperature from room temperature (ramp rate= 20 °C/min) to 200 °C. The sample was then cooled to room temperature and subsequently heated to 1000 °C at 10 °C/min in a flow (50 ml/min) of pure H_2. The amount of hydrogen consumed during reduction was measured with a thermal conductivity detector (TCD). Simultaneously, the off-gas was analysed using the MS for all masses between 1 and 50.

3. Results and discussion

3.1. XANES analysis of reference compounds

Fig. 2 shows XANES analyses of cobalt reference compounds CoO, Co_3O_4, $CoAl_2O_4$, and cobalt foil (Co^0). The oxidic reference compounds display a strong absorption white line with unique spectral features due to the presence of cobalt atoms in different Co–O environments and oxidation states. The XANES spectra of the oxides also display a small pre-edge feature (ca. 7710 eV). This pre-edge feature arises from the 1s-3d absorption transition and appears most strongly for tetrahedral cobalt environments as compared to octahedral environments [42]. CoO consists of Co^{2+} ions octahedrally coordinated to oxygen, whereas Co_3O_4 has a spinel type structure with both tetrahedral Co^{2+} and octahedral Co^{3+} ions [42]. $CoAl_2O_4$ is a normal spinel with Co^{2+} ions in tetrahedral sites [43]. Hence, this pre-edge feature is most pronounced for $CoAl_2O_4$ and Co_3O_4. It is clear from Fig. 2 that using XANES it is easy to distinguish between Co^0, CoO and Co_3O_4 and to a lesser extent $CoAl_2O_4$. However if we use the derivative spectrum (Fig. 3), it is clear that the CoO and $CoAl_2O_4$ are more distinguishable.

3.2. Study of aluminate formation during extended demonstration unit FTS run

It was previously shown [14] that $Co/Pt/Al_2O_3$ catalysts tested in a 100 bbl/day slurry bubble column reactor, under realistic conditions (230 °, 20 bar, H_2 + CO conversion between 50 and 70%, feed gas composition of 50–60 vol.% H_2 and 30–40 vol.% CO) undergo deactivation during the course of the run which could be due to many factors. As mentioned earlier the presence of reaction water at partial pressures of 4–6 bar may be one of the factors that could lead to catalyst deactivation. XANES analysis of catalyst samples was done to observe whether cobalt aluminate was formed. Fig. 4 shows that during the course of the reaction the catalyst does not undergo any oxidation but is instead reduced as the XANES spectrum of samples closely resembles the spectrum of a Co foil. The observed behaviour for >6 nm Co particles (at $P_{H_2O}/P_{H_2} = 1–1.5$, $P_{H_2O} = 4–6$ bar) is in line with previous work [22] and also supported by thermodynamic calculations [44]. Furthermore the derivative spectrum (Fig. 5) shows that a minimal amount of cobalt aluminate is formed which is in the error of the fitting. Hence, at these conditions, with water partial pressure of 4–6 bar, cobalt aluminate formation is not that significant (Table 1) and cannot account for the deactivation observed in the extended run [14]. We could not detect cobalt–aluminate in the freshly reduced catalyst within the sensitivity of the XANES measurement. Due to the strongly reducing environment during FTS and the observed reduction of CoO to Co(0) during FTS, it is unlikely that the formed cobalt aluminate originates from the cobalt metal (i.e. Co(0)). The observed cobalt aluminate arises most likely from

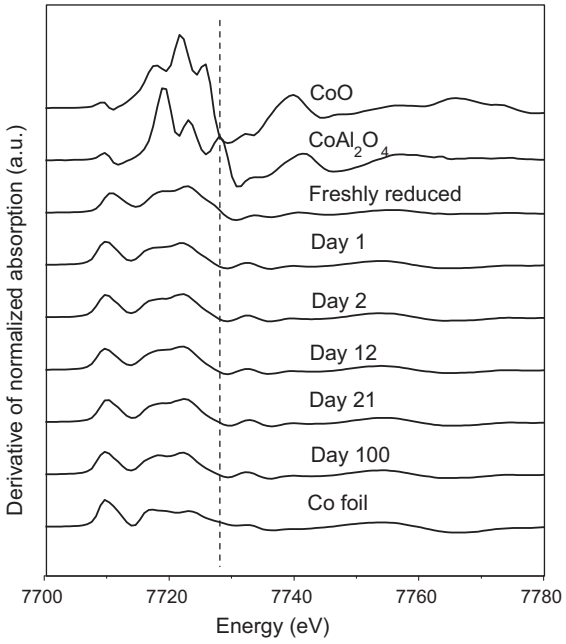

Fig. 5. XANES derivative spectra of $Co/Pt/Al_2O_3$ catalysts taken at different intervals from an extended FTS run and compared to reference compounds.

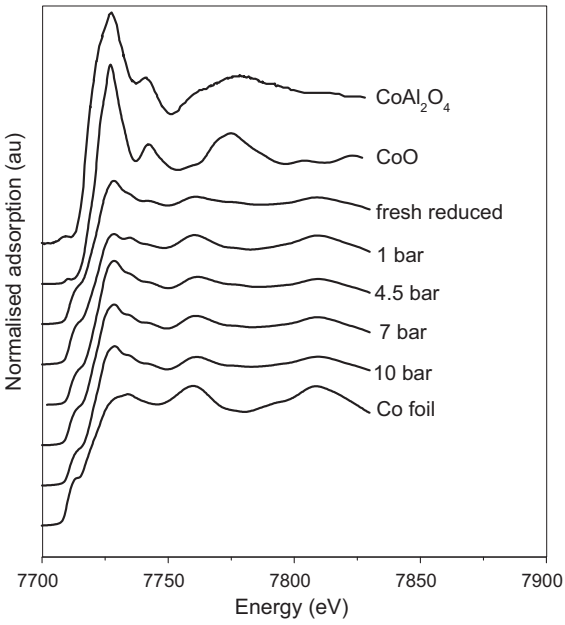

Fig. 6. Co K-edge spectra showing the influence of varying water partial pressures on $Co/Pt/Al_2O_3$ catalysts.

the reaction of the unreduced cobalt oxide with the alumina support and this should have no influence on the deactivation of the catalyst.

3.3. Runs with varying water partial pressure

3.3.1. XANES analysis of samples tested at various water partial pressures

FTS runs were carried out in laboratory CSTR at 230 °C, 10–20 bar, where the water partial pressure was varied between 1 and 10 bar. This was done in order to observe if higher water partial pressures, will result in aluminate formation. The initial activities for the catalysts tested at the various water partial pressures were similar. Depending on the support, different results on the effect of water on catalyst activity have been reported [45]. For Co/Al_2O_3 catalysts it is known that high water partial pressures result in decreased activity and this is ascribed to oxidation and aluminate formation [11,28]. Under our conditions the oxidation of cobalt is not observed with XANES (Fig. 6). XANES analyses showed that at higher water partial pressures (i.e. >6 bar) the catalyst still underwent reduction compared to the fresh catalyst, which is in line with thermodynamics. Interestingly at higher water partial pressures the amount of cobalt aluminate increased. From the quantification (Table 2) it can be seen that cobalt aluminate is formed at the expense of the cobalt oxide and not the metal. Even at high water partial pressures ($P_{H_2O} = 10$ bar, $P_{H_2O}/P_{H_2} = 2.2$), a reduction is observed of CoO to Co(0) when compared to a freshly reduced catalyst. Bulk thermodynamic data indicates that at these conditions the reduction of CoO to Co should be spontaneous at P_{H_2O}/P_{H_2} below 50 [46]. It must be stated that most of the CoO exists as 2–3 nm crystallites [23] and these small particles are expected to have a strong interaction with the support and may be difficult to reduce. The derivative spectrum (Fig. 7) indicated that only small amounts of cobalt aluminate are formed (≤10%) even at higher water partial pressures. To confirm this result that aluminate does indeed form, we performed different linear combinations (containing various amounts of Co, CoO and aluminate) and compared them to the derivative 10 bar spectrum. It can clearly be seen that the 10 bar sample does contain cobalt–aluminate and not just Co metal and CoO (Fig. 8).

3.3.2. XPS analysis of samples with varying water partial pressure

Four catalyst samples were analysed by XPS with the aim of observing changes in surface composition that may occur during FTS conducted with higher water partial pressures. The samples included a freshly reduced catalyst and catalysts treated at 4.5 and 10 bar water partial pressures. The wax covered samples were first extracted with THF at mild extraction conditions (~66 °C in Ar) using a P25 frit (16–40 μm) and this treatment is not expected to cause any change in the amount of cobalt aluminate in the catalysts. The catalysts were then passivated in a glove box. Passivation is expected to create a layer of CoO. These were then transferred under a protective atmosphere into the XPS set-up.

When comparing the Co 2p region of the XPS presented in Table 3, it can be seen that the Co $2p_{3/2}$ peak positions for the 10 bar sample seem to be shifted to higher binding energies compared to

Table 1
Quantification of XANES analyses of a series of $Co/Pt/Al_2O_3$ catalysts tested during realistic FTS in a 100 bbl/day slurry bubble column, using a linear combination of reference compounds. Error = ±3%. Mol.% of total cobalt is shown.

Sample	Co^0 (%)	CoO (%)	$CoAl_2O_4$ (%)
Freshly reduced	58	42	–
Day 1	84	16	–
Day 2	86	12	2
Day 21	86	11	3
Day 100	87	11	2

Table 2
Quantification of XANES analyses of a series of $Co/Pt/Al_2O_3$ catalysts exposed to varying water partial pressures during FTS (10–20 bar, 230 °C) taken from a laboratory CTSR using a linear combination of reference compounds. Error = ±3%. Mol.% of total cobalt is shown.

Sample	H_2O/H_2	Co^0 (%)	CoO (%)	$CoAl_2O_4$ (%)
Freshly reduced	–	58	42	–
1 bar	0.2	88	12	–
4.5 bar	1	74	23	3
7 bar	1.6	73	18	9
10 bar	2.2	72	18	10

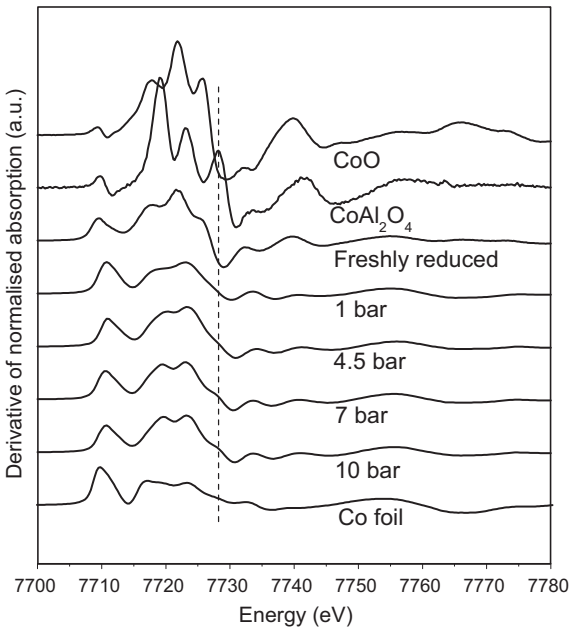

Fig. 7. XANES derivative spectra of $Co/Pt/Al_2O_3$ catalysts exposed to varying water partial pressures compared to reference compounds. The slight evolution of cobalt aluminate can be noted at higher water partial pressures (shoulder at 7728 eV).

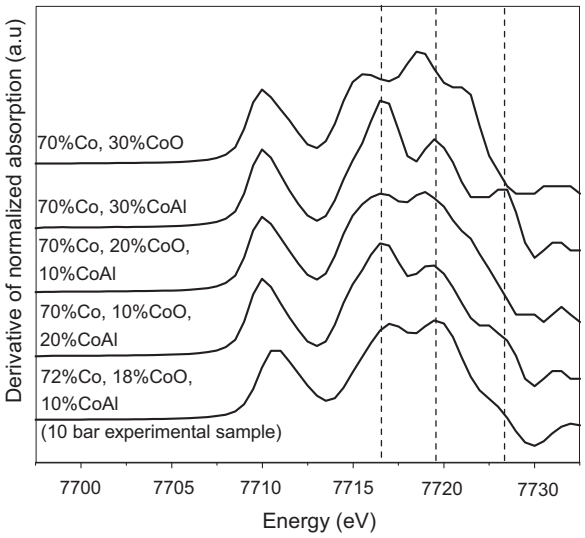

Fig. 8. Linear combinations of various amounts of Co, CoO and $CoAl_2O_4$ compared to the 10 bar experimental sample. The dashed lines represent derivative maxima from different $Co/CoO/CoAl_2O_4$ mixtures.

Table 3
Co $2p_{3/2}$ binding energy, shake-up satellite position, doublet separation (DS) values for Co $2p_{3/2}$ and Co $2p_{1/2}$ components and Al 2p binding energy of reference compounds, wax-extracted freshly reduced catalyst and catalysts tested at 4.5 and 10 bar water partial pressures.

Sample	Co $2p_{3/2}$ (eV)	Shake-up satellite (eV from main photoline)	DS (eV)	Al 2p (eV)
Freshly Reduced	780.9	5.0	16.0	74.4
4.5 bar	781.1	5.3	15.7	74.3
10 bar	781.0	5.1	15.5	74.1
CoO	780.5*	5.8	15.5	–
$CoAl_2O_4$	780.9*	5.5	15.5	74.1

* Measured in-house.

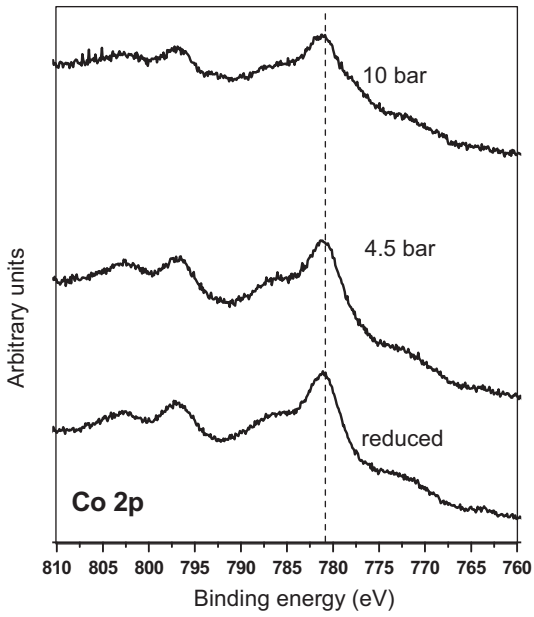

Fig. 9. XPS Co2p spectra of wax-extracted samples of freshly reduced and $Co/Pt/Al_2O_3$ catalysts exposed to increasing water partial pressure.

the reduced catalyst. The binding energy and doublet separation information (Table 3) along with the fact that the spectra show strong shake-up features (about 5–6 eV from main peak) gives an indication that the samples contain cobalt compounds in high spin states e.g. CoO and $CoAl_2O_4$. Unfortunately by using the Co 2p XPS region only (Fig. 9), it is extremely difficult to differentiate between the CoO and cobalt aluminate for the extracted samples.

However, the Al 2p region of the XPS spectra can possibly provide information in support of XANES, with regards to cobalt aluminate formation. The Al 2p peak position of the reduced catalyst (Table 3) corresponds more closely with Al_2O_3, which has a value of 74.4 eV [47]. This peak shifts to lower binding energies for samples exposed to higher water partial pressure. This decrease in the Al 2p binding energy possibly points to the formation of a cobalt aluminate support compound. The Al 2p position in a $CoAl_2O_4$ reference sample was determined to be 74.1 eV. Although the amount of cobalt aluminate formed is small ($\lesssim$10%), there is considerable shift in the binding energies of the Al 2p peak. This may be explained by the premise that cobalt aluminate formation results in the flattening out of a particle over the support surface, resulting in an increased sensitivity in XPS.

3.3.3. TPR-MS analysis of a spent sample varying water partial pressure

To further confirm the results from XANES and XPS, TPR-MS analysis was performed on a spent catalyst operated for 7 days-on-line at 10 bar water partial pressure in a microslurry reactor and results were compared to a pure $CoAl_2O_4$ sample and the spent sample which was operated at $P_{H_2O} = 4.5$ bar (Fig. 10). It must be noted that the spent catalyst samples did undergo controlled wax-extraction, hydrocracking (350 °C) and oxidation (250 °C) prior to the TPR measurement to remove carbon (around 1–2 wt% carbon remains), although these treatments are not expected to alter cobalt aluminate formation on the samples. For the spent oxidised catalysts, the two reduction steps of Co_3O_4 ($Co_3O_4 \rightarrow CoO \rightarrow Co$) which is the main phase expected in the catalyst are observed as the main two peaks at around 300 and 450 °C. Hydrogen is also consumed in the region between 200 and 500 °C due to the methanation of residual carbon (see Fig. 11) which will also influence the

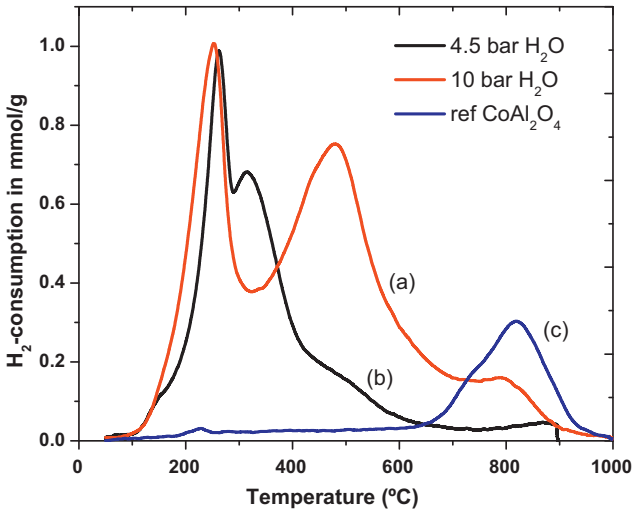

Fig. 10. TPR profiles of a spent catalyst after FTS at (a) 10 bar and (b) 4.5 bar water partial pressure. *Note*: a TPR pattern of pure $CoAl_2O_4$ (c) is included as reference.

TPR pattern slightly. The $CoAl_2O_4$ reference sample is only reduced at around 700–950 °C.

A peak in the temperature range of 800–1000 °C could be obtained for the spent sample operated at $P_{H_2O} = 10$ bar and for the spent sample operated at $P_{H_2O} = 4.5$ bar. These peaks are in alignment with the single reduction peak of pure $CoAl_2O_4$. The MS pattern (Fig. 11) of the spent sample operated at $P_{H_2O} =$ 10 bar showed indeed the formation of H_2O ($m/e = 17$), whereas no methane formation ($m/e = 15$) was obtained in this temperature range. Therefore, this high temperature peak does not result from hydrocracking of a highly graphitic C-species, but rather from the reduction of $CoAl_2O_4$. It must be noted that we could not detect a significant cobalt–aluminate type peak in a fresh (unused) catalyst.

By comparing the areas under the $CoAl_2O_4$ peaks of the spent catalyst operated at 10 bar P_{H_2O} to the spent catalyst operated at 4.5 bar P_{H_2O}, a 3:1 ratio was obtained. Deconvolution of the water signal in Fig. 10 indicated that about 8% of area for the 10 bar sample corresponds to reduction of $CoAl_2O_4$.This is in agreement with XANES results indicating approximately three times more $CoAl_2O_4$ formation at 10 bar water partial pressure in contrast to a spent sample operated at baseline conditions of 4.5 bar.

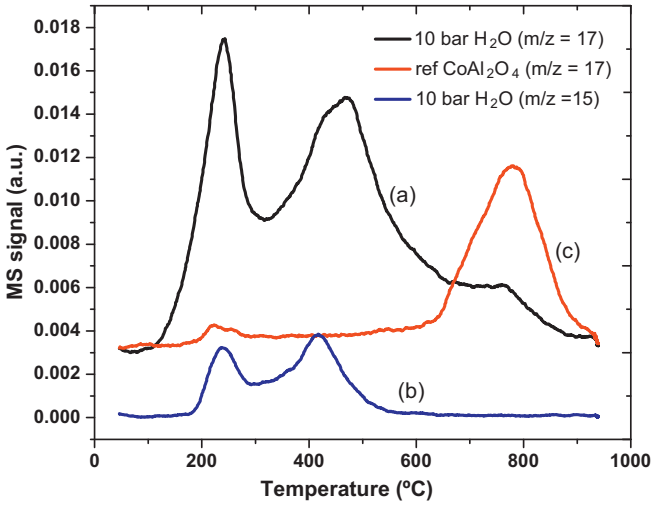

Fig. 11. MS patterns for (a) H_2O ($m/z = 17$) and (b) CH_4 ($m/z = 15$) during the TPR of a spent catalyst after FTS at 10 bar water partial pressure. *Note*: a MS profile of H_2O ($m/z = 17$) for the reduction of pure $CoAl_2O_4$ (c) is included as reference.

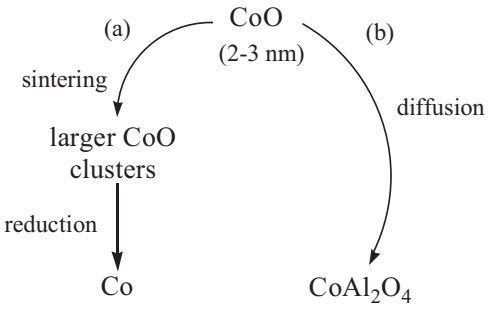

Scheme 1. Possible pathways for formation of metallic cobalt and cobalt aluminate from CoO. The hypothesis is that pathway (a) is favoured over (b).

4. Proposed mechanism of reduction and aluminate formation

It is clear from the XANES measurements that CoO undergoes a reduction during the extended FTS run at commercially relevant conditions and aluminate formation is not observed to a great extent. This reduction behaviour was reported previously by Saib et al. [22] for cobalt catalysts tested in a slurry bubble column under similar conditions, which shows that strong reducing nature of the FT environment. Oosterbeek [48] also showed the strong reduction tendency of cobalt oxide under synthesis conditions. He observed the complete reduction of a highly oxidic Co(poly) crystal under FT conditions with XPS. Den Breejen et al. [49] recently observed an increase in reduction extent for Co/SiO_2 catalysts during the first few hours of FTS.

In the case of catalysts exposed to higher water partial pressures compared to realistic FTS conditions, we still observe a reduction compared to the fresh catalyst and cobalt aluminate formation in the order of 10%. This is in line with thermodynamic expectations. Based on the quantification it is proposed that this aluminate is formed from existing 2–3 nm CoO clusters and not from metallic cobalt as an increase in the reduction extent is observed from the fresh catalyst. To explain the co-current observation of CoO reduction to Co(0) as well as $CoAl_2O_4$ formation we propose the following (Scheme 1): (a) relatively quick sintering of small CoO crystallites to form larger clusters, with a relatively weakened inter-

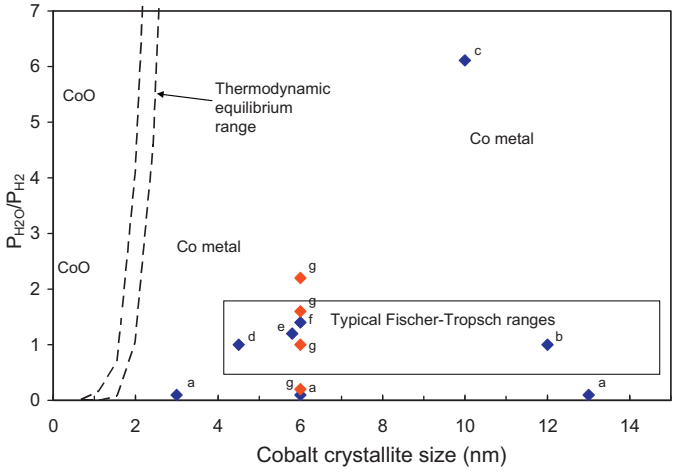

Fig. 12. Reconciliation of the effect of the water/hydrogen reactor ratio as a function of cobalt crystallite size on the oxidation behaviour of cobalt (a [9], b [55], c [8], d [56], e [22], f [57] and g from the current study). All the data are superimposed on the thermodynamic equilibrium data range [54].
Adapted from [15].

action with the support, which are then reduced; and (b) a slower process involving the formation of cobalt aluminate from interaction of CoO with the support which could be enhanced by water. It should be noted that the reduction mechanism of CoO is only a postulate at this stage and this needs further study.

As mentioned earlier, it is expected that the small CoO crystallites have a strong interaction with the support. However water is known to affect the interface energy between the support and crystallites and the dynamic gas environment that exists can drive the sintering process [50]. Once the CoO crystallites sinter to above 4–5 nm then it is thermodynamically [44] and possibly kinetically favourable for them to be transformed to Co in the highly reducing H_2/CO environment [51].

The formation of cobalt aluminate is known to proceed via CoO as an intermediate [7]. The presence of water can result in hydration of the alumina support as reported by Oukaci and co-workers [52]. The hydrated alumina appears to enhance the diffusion of small CoO particles in strong interaction with the support, during prolonged treatment resulting in the formation of non-reducible cobalt aluminate. This may explain why small amounts of aluminate are formed in the case of catalyst exposed to higher water partial pressures [52]. It is expected that this is a kinetically slow process as it involves diffusion into the support [53]. It is therefore believed that the sintering/reduction process (a) is favoured over the transformation of CoO into aluminate (b).

We have used this knowledge (i.e. that $CoAl_2O_4$ originates from CoO and not Co(0)) to update the oxidation figure [15] that shows the possibility of oxidation as function of crystallite size and H_2O/H_2. Therefore, data from literature that reported on the formation of cobalt-aluminate and/or cobalt–silicate were removed, as our renewed understanding is that these cobalt-support compounds are formed from existing unreduced cobalt oxide and not from cobalt metal that was oxidized. We have updated this reconciliation (see Fig. 12) with revised thermodynamic calculations from Swart [54], who showed that the surface energy for cobalt oxide was previously [44] underestimated. The data from this study using a varying H_2O/H_2 ratio were of course also added to that shown in earlier work [8,9,22,55,56].

The observed deactivation in the demonstration unit can thus not be explained by oxidation or aluminate formation. The reduction to Co metal should have resulted in an increase in intrinsic catalyst activity however this was not the case. The deactivation is most likely due to a complex interplay of other deactivation mechanisms such as sintering [37] of metallic crystallites (enhanced by water) and carbon deposition [14] both of which were demonstrated for this particular run. These factors may overshadow the effect of CoO reduction.

5. Conclusions

During this study we showed that XANES can distinguish between CoO, $CoAl_2O_4$ and Co^0 in wax-coated cobalt on alumina FTS catalysts, taken from a 100 bbl/day slurry bubble column reactor, with reasonable sensitivity. We did not observe oxidation of >6 nm Co crystallites at P_{H_2O}/P_{H_2} ratios up to 2.2 but instead reduction of CoO was noted. The amount of cobalt aluminate formed was small and it appears that its formation is difficult during FTS (surface and bulk). Water does seem to enhance aluminate formation but at high water partial pressure (10 bar) around 10% cobalt aluminate was formed and a reduction was observed compared to a fresh catalyst. However, it should be noted that this amount of cobalt aluminate was formed after a short time on stream at 10 bar and running the reaction for longer periods at these high water partial pressures could result in further aluminate formation. The cobalt aluminate that did form resulted from existing CoO.

This leads us to the conclusion that small amounts of cobalt aluminate formation does not influence deactivation of cobalt catalysts during *realistic* FTS conditions (P_{H_2O}/P_{H_2} = 1–1.5, P_{H_2O} = 4–6 bar). The observed deactivation is due to an interplay between other phenomena which includes, sintering of cobalt crystallites, surface reconstruction, and carbon deposition which have been reported earlier for this particular run.

Acknowledgements

The authors would like to thank Mr. Tiny Verhoeven, Dr Esna du Plessis and Dr. Ionel Ciobîcă for assistance during XANES measurements.

References

[1] R. Zennaro, Oil Gas 2 (2007) 88.
[2] Fischer–Tropsch technology, in: A.P. Steynberg, M.E. Dry (Eds.), in: Studies in Surface Science and Catalysis, vol. 152, Elsevier, 2004.
[3] E. Iglesia, Appl. Catal. A 161 (1997) 59.
[4] M.E. Dry, Appl. Catal. A 276 (2004) 1.
[5] C.H. Bartholomew, R.M. Bowman, Appl. Catal. 15 (1985) 59.
[6] J. Inga, P. Kennedy, S. Leviness, United States Patent Application 20050154069 A1 (2004) to Syntroleum.
[7] P.J. van Berge, J. van de Loosdrecht, S. Barradas, A.M. van der Kraan, Catal. Today 58 (2000) 321.
[8] G.Z. Bian, N. Fujishita, T. Mochizuki, W.S. Ning, M. Yamada, Appl. Catal. A 252 (2003) 251.
[9] G.L. Bezemer, J.H. Bitter, H.P.C.E. Kuipers, H. Oosterbeek, J.E. Holewijn, X. Xu, F. Kapteijn, A.J. van Dillen, K.P. de Jong, J. Am. Chem. Soc. 128 (2006) 3956.
[10] J. Wilson, C. de Groot, J. Phys. Chem. 99 (1995) 7860.
[11] Y. Li, G. Jacobs, T. Das, B.H. Davis, Appl. Catal. A 228 (2002) 203.
[12] G. Kiss, C. Kliewer, G.J. DeMartin, C.C. Culross, J.E. Baumgartner, J. Catal 217 (2003) 127.
[13] V. Gruver, R. Young, J. Engman, H.J. Robota, Prepr. Pap. -Am. Chem. Soc., Div. Pet. Chem. 50 (2005) 164.
[14] D.J. Moodley, J. van de Loosdrecht, A.M. Saib, M.J. Overett, A.K. Datye, J.W. Niemantsverdriet, Appl. Catal. A 354 (2009) 102.
[15] A.M. Saib, D.J. Moodley, I.M. Ciobîcă, M.M. Hauman, B.H. Sigwebela, C.J. Weststrate, J.W. Niemantsverdriet, J. Van de Loosdrecht, Catal. Today 154 (2010) 271.
[16] J. van de Loosdrecht, S. Barradas, E.A. Caricato, N.G. Ngwenya, P.S. Nkwanyana, M.A.S. Rawat, B.H. Sigwebela, P.J. van Berge, J.L. Visagie, Top. Catal. 26 (2003) 121.
[17] R. Oukaci, A.H. Singleton, J.G. Goodwin Jr., Appl. Catal. A 186 (1999) 129.
[18] F. Dumond, E. Marceau, M. Che, J. Phys. Chem. C 111 (2007) 4780.
[19] W. Chu, P.A. Chernavskii, L. Gengembre, G.A. Pankina, P. Fongarland, A.Y. Khodakov, J. Catal. 252 (2007) 215.
[20] B. Jongsomjit, J. Panpranot, J.G. Goodwin Jr., J. Catal. 204 (2001) 98.
[21] W.J. Wang, Y.W. Chen, Appl. Catal. 77 (1991) 223.
[22] A.M. Saib, A. Borgna, J. van de Loosdrecht, P.J. van Berge, J.W. Niemantsverdriet, Appl. Catal. A 312 (2006) 12.
[23] P.H. Bolt, PhD thesis, University of Utrecht, The Netherlands, 1994.
[24] R.B. Anderson, in: P.H. Emmett (Ed.), Catalysis, vol. 4, Reinhold, New York, 1956.
[25] D. Schanke, A.M. Hilmen, E. Bergene, K. Kinnari, E. Rytter, E. Ådnanes, A. Holmen, Catal. Lett. 345 (1995) 269.
[26] G. Jacobs, T.K. Das, P.M. Patterson, J. Li, L. Sanchez, B.H. Davis, Appl. Catal. A 247 (2003) 335.
[27] G. Jacobs, P.M. Patterson, Y. Zhang, T. Das, J. Li, B. Davis, Appl. Catal. A 233 (2002) 215.
[28] A.M. Hilmen, D. Schanke, K.F. Hanssen, A. Holmen, Appl. Catal. A 186 (1999) 169.
[29] A. Tavasoli, A. Nakhaeipour, K. Sadaghiani, Fuel Proc. Technol. 88 (2007) 461.
[30] N.E. Tsakoumis, M. Rønning, Ø. Borg, E. Rytter, A. Holmen, Catal. Today 154 (2010) 162.
[31] P.J. van Berge, J. van de Loosdrecht, J.L. Visagie, United States Patent 6 806 226, 2004, to Sasol.
[32] P.J. van Berge, J. van de Loosdrecht, E. Caricato, S. Barradas, B.H. Sigwebela, United States Patent 6 455 462, 2002, to Sasol.
[33] P.J. van Berge, J. van de Loosdrecht, E. Caricato, S. Barradas, United States Patent 6 638 889, 2004, to Sasol.
[34] R.L. Espinoza, J.L. Visagie, P.J. van Berge, F.H. Bolder, United States Patent 5 733 839, 1998, to Sasol.
[35] P.J. van Berge, J. van de Loosdrecht, J.L. Visagie, T.J. van der Walt, H. Veltman, C. Sollie, European Patent 1 444 040 B1, 2003, to Sasol.
[36] P.J. van Berge, J. van de Loosdrecht, J.L. Visagie, United States Patent 6 385 690, 2004, to Sasol.
[37] M.J. Overett, B. Breedt, E. du Plessis, W. Erasmus, J. van de Loosdrecht, Prepr. Pap. -Am. Chem. Soc., Div. Petr. Chem, 53 (2008) 126.
[38] C.A. Chanenchuk, I.C. Yates, C.N. Satterfield, Energy Fuels 5 (1991) 847.
[39] I.C. Yates, C.N. Satterfield, Energy Fuels 5 (1991) 168.
[40] H. Schulz, A. Geertsema, Erdöl und Kohle 20 (1985) 38.

[41] http://csrri.iit.edu/cgi-bin/period-form?ener=&name=Co (accessed on 21 October 2010).
[42] D. Bazin, I. Kovacs, L. Guczi, P. Parent, C. Laffon, F. de Groot, O. Ducreux, J. Lynch, J. Catal. 189 (2000) 456.
[43] M. Zayat, D. Levy, Chem. Mater. 12 (2000) 2763.
[44] E. van Steen, M. Claeys, M. Dry, E. Viljoen, J. van de Loosdrecht, J.L. Visagie, J. Phys. Chem. B 109 (2005) 3575.
[45] Ø. Borg, S. Storsæter, S. Eri, H. Wigum, E. Rytter, A. Holmen, Catal. Lett. 107 (2006) 95.
[46] J.W. Niemantsverdriet, Spectroscopy in Catalysis: An Introduction, 3rd ed., Wiley-VCH, Weinheim, 2007, p. 14.
[47] N.S. McIntyre, M.G. Cook, Anal. Chem. 47 (1975) 2208.
[48] H. Oosterbeek, Phys. Chem. Chem. Phys. 9 (2007) 3570.
[49] J.P. den Breejen, J.R.A. Sietsma, H. Friedrich, J.H. Bitter, K.P. de Jong, J. Catal. 270 (2010) 146.
[50] P. Hansen, J.B. Wagner, S. Helveg, J.R. Rostrup-Nielsen, B.S. Clausen, H. Topsøe, Science 295 (2002) 2053.
[51] A.M. Saib, PhD thesis, Eindhoven University of Technology, The Netherlands, 2006.
[52] A. Sirijaruphana, A. Horvath, J.G. Goodwin Jr., R. Oukaci, Catal. Lett. 91 (2003) 89.
[53] P.H. Bolt, F.H.P.M. Habraken, J.W Geus, J Solid State Chem. 135 (1998) 59.
[54] J.C.W. Swart, Ph.D. thesis, University of Cape Town, South Africa, 2008.
[55] N.O. Elbashir, P. Dutta, A. Manivannan, M.S. Seehra, C.B. Roberts, Appl. Catal. A: Gen. 285 (2005) 169–180.
[56] A.M. Saib, A. Borgna, J. van de Loosdrecht, P.J. van Berge, J.W. Niemantsverdriet, J. Phys. Chem. B 110 (2006) 8657.
[57] J. van de Loosdrecht, B. Balzhinimaev, J.-A. Dalmon, J.W. Niemantsverdriet, S.V. Tsybulya, A.M. Saib, P.J. van Berge, J.L. Visagie, Catal. Today 123 (2007) 293.